JOURNAL OF SPACECRAFT AND ROCKETS
Vol. 31, No. 5, September–October 1994

Acceleration Mapping on Consort 5

Robert J. Naumann*
University of Alabama in Huntsville, Huntsville, Alabama 35812

The Consort 5 rocket carrying a set of commercial low-gravity experiments experienced a significant side thrust from an apparent burn-through of the second-stage motor just prior to cut-off. The resulting angular momentum could not be removed by the attitude rate control system, thus the payload was left in an uncontrollable rocking/tumbling mode. Although the primary low-gravity emphasis mission requirements could not be met, it was hoped that some science could be salvaged by mapping the acceleration field over the vehicle so that each investigator could correlate his or her results with the acceleration environment at his or her experiment location. This required some detective work to obtain the body rates and moment of inertia ratios required to solve the full set of Euler equations for a tri-axial rigid body. The techniques for acceleration mapping described in this paper may be applicable to other low-gravity emphasis missions.

Nomenclature

$\mathbf{a}$	= acceleration vector, m/s
B	= I_2/I_1
C	= I_3/I_1
KE	= rotational kinetic energy, J
$\mathbf{L}$	= angular momentum vector, kg m^2/s
I_1, I_2, I_3	= moments of inertia about the principle axes of greatest, intermediate, and least moment of inertia, kg m^2
$\mathbf{r}$	= position vector in body coordinates, m
x, y, z	= vehicle coordinates; x is centerline from top of the payload section; y is toward the launch rail, and z is normal to experiment mounting plates
ν	= angle from the vehicle y-axis to the principle axis of greatest moment of inertia
ω	= angular velocity vector in body-fixed coordinates, rad/s

Introduction

CONSORT 5 was the fifth in a series of suborbital low-gravity missions managed by the Consortium for Materials Development in Space at the University of Alabama in Huntsville (UAH). The vehicle was an EER, Inc., Starfire rocket, which is comprised of a Thiokol TX 664-5 (derived from the Terrier Mk 12 motor) booster and a Bristol Aerospace Black Brant VC second stage[1] (see Fig. 1). Typically, a 300-kg payload package containing approximately a dozen experiments is boosted to around 300 km, giving just under 7 min of microgravity time during which the effective g-levels from atmospheric drag are below 10 μg. The vehicle is spun during the boost phase for stability. Just after second stage burn-out, a yo-yo de-spin device is deployed, and cold gas thrusters controlled by three rate gyros null out any residual body rates to ensure less than 10 μg everywhere in the payload compartment.

After a completely nominal launch, the Black Brant apparently suffered a casing burn-through just a few seconds before its scheduled burn-out. The final velocity was slightly less than planned, but was sufficient to give nearly 6 minutes of low-g time. However, the impulse (estimated to be in excess of 100 g for 1 ms) from the burn-through applied a significant side force to the vehicle, causing it to begin to cone and tumble. The impulse also caused the de-spin yo-yos to deploy prematurely, one of which apparently wrapped around the payload, as evidenced by cable marks on the skin. The cold gas thrusters attempted to null the body rates, but the gas supply became exhausted before this could be accomplished. This left the payload gyrating about its center of mass in a combination end-over-end tumble and rocking motion about its cylindrical axis. The centrifugal accelerations from these motions prevented the experiments from achieving their desired levels of microgravity. In order to salvage as much science as possible from the flight, it was desirable to be able to provide each experimenter with the acceleration environment at his or her experiment location. If the time-varying, body-fixed angular velocity vector ω was known, the centrifugal acceleration at any location could be obtained from

$$\boldsymbol{a} = -[\omega \times (\omega \times \mathbf{r}) + \dot{\omega} \times \mathbf{r}] \tag{1}$$

The problem was made difficult because the constants of motion (i.e., the angular momentum and the rotational kinetic energy) were not known. To make matters worse, the rate gyros were damaged by the impulse and were unable to supply useful data.

The SAAB S-19 package, which provides guidance during the first 18 s of flight when the vehicle is in the sensible atmosphere, contains two reference gyros mounted on gimbal rings, which, in turn, are mounted on a servocontrolled Midas platform that can rotate about the vehicle's x-axis. This allows the platform to remain inertially stable while the vehicle spins about the x-axis during the boost phase. The pitch gyro provides an inertial reference direction and was initially aligned with the vehicle's x-axis. An optical pick-off measures the angle the platform axis, hence the vehicle's x-axis, makes with this reference direction. The yaw/roll gyro axis provides a second orthogonal reference direction. One optical pick-off measures the yaw angle, and a second pick-off drives the roll servo. The roll angle is measured by a pick-off on the axis of the Midas platform. Because this package is designed to operate only during a period when pitch and yaw deviations are expected to be small, full scale on the telemetry output for these angles was set at ±28 deg deflection.

Although the S-19 package is used only for the first 18 s of flight, the gyros continued to function throughout the remainder of the mission. The pitch data exhibited a clipped, saw-toothed behavior with a 4.70-s period indicating a continuously increasing angle corresponding to an average rate of 76 deg/s or 1.34 rad/s, as seen in Fig. 2. The yaw output appeared as a clipped sine wave, indicating a oscillation with the same period; however, because the peak angular displacement was off-scale, the amplitude could not be determined. The roll could be determined directly from the roll gyro and exhibited an oscillatory motion with an amplitude of ±15 deg and a period of 19 s.

The vehicle was also equipped with two single-axis magnetometers to provide an independent determination of roll rate during the boost phase. The pitch axis magnetometer, whose axis is aligned

Received May 14, 1993; revision received Aug. 27, 1993; accepted for publication Aug. 27, 1993.

*Professor of Materials Science, Department of Materials and Science. Member AIAA.

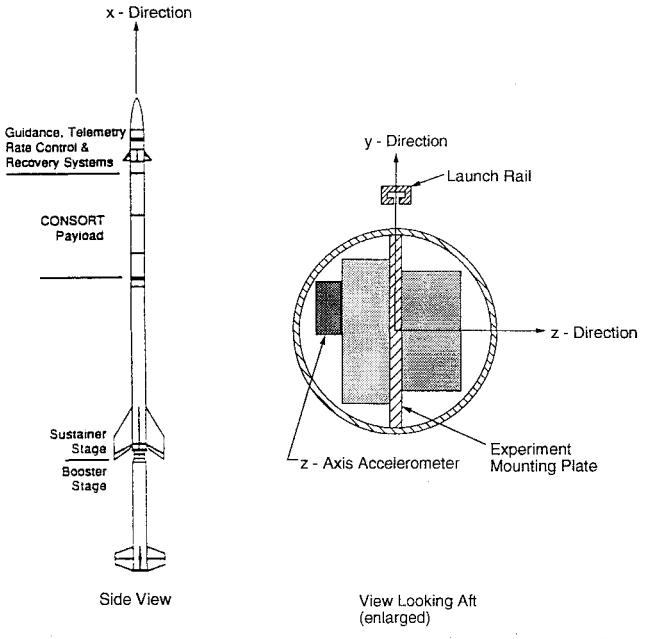

Fig. 1 Schematic of the Starfire vehicle showing the vehicle coordinate system and placement of the z-axis accelerometer.

along the vehicle's x-axis, showed a sinusoidal signal with a period of 4.7 s. The yaw axis magnetometer, whose axis is perpendicular to the vehicle's x-axis, also produced a sinusoidal output with a period of 4.7 s, but the amplitude was modulated with a period of 19 s. Because the magnetometers were never intended to provide absolute angular data relative to the local magnetic field, they were not calibrated. In addition, the orientation of the vehicle angular momentum vector was not known relative to the magnetic field vector. However, the magnetometer data are qualitatively consistent with the motions deduced from reference gyros; thus, they provide an independent check on the interpretation of the reference gyro data.

The payload was also equipped with a three-axis accelerometer,[2] which provided an acceleration history at one particular location. This allows a direct comparison of the acceleration calculated from the rates deduced from the gyros with the measured acceleration at one point. This comparison can also be used to ascertain the orientation of the principal axes relative to the vehicle coordinates.

The payload was in the shape of a long, thin cylinder of approximately 4 m length and 0.43 m diam. The ratio of the moment of inertia about the cylindrical axis to the moment of inertia about a transverse axis was determined to be 0.009. Because the payload is essentially a cylinder, for most purposes it had been sufficient to treat it as a symmetrical body of revolution. Therefore, no effort was made prior to launch to determine the moments of inertia about the transverse principal axis or to identify these principal axes relative to the vehicle coordinates.

However, because the reduced set of Euler equations for a slender symmetrical cylindrical body do not permit oscillatory motion about the axis of symmetry, the fact that the vehicle was apparently executing a complex rocking and tumbling motion indicated that the transverse moments of inertia were distinct, and the solution to the full set of Euler equations for a triaxial rigid body would be required to describe the vehicle's motion. This solution is extremely sensitive to the ratio I_2/I_1, which had not been measured prior to flight. Furthermore, the mass properties of the vehicle were not known accurately enough to compute this ratio to the required precision. Also, there was the possibility that the de-spin yo-yo was still wrapped around the vehicle. Thus, in order to solve the problem, a set of conditions had to be found for which the solution of Euler equations produced the accelerations observed by the three-axis accelerometer. This solution could then be used to compute the acceleration vector at the location of any other experiment package by using Eq. (1).

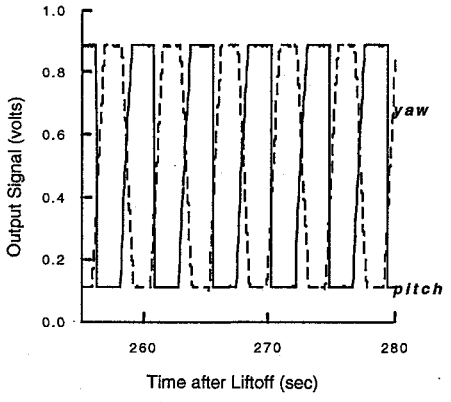

Fig. 2 Observed output from the S-19 pitch and yaw gyros. The data are clipped at ±28 deg, which corresponds to 0.1 and 0.9 volts output.

Analysis

The full set of Euler equations for a force-free triaxial rigid body may be written as

$$\begin{aligned} I_1\dot{\omega}_1 &= (I_2 - I_3)\omega_2\omega_3 \\ I_2\dot{\omega}_2 &= (I_3 - I_1)\omega_3\omega_1 \\ I_3\dot{\omega}_3 &= (I_1 - I_2)\omega_1\omega_2 \end{aligned} \tag{2}$$

External torque from drag or gravity gradient effects would produce changes in angular momentum that are orders of magnitude smaller than those appearing in Eq. (2). Therefore, the use of the force-free formulation is justified.

The constants of motion are L and KE, which are given by

$$\begin{aligned} L^2 &= I_1^2\omega_1^2 + I_2^2\omega_2^2 + I_3^2\omega_3^2 \quad \text{and} \\ 2KE &= I_1\omega_1^2 + I_2\omega_2^2 + I_3\omega_3^2 \end{aligned} \tag{3}$$

The solution to this set of equations takes two different forms, depending on the relationship between KE, L, and I_2. If $L^2 > 2I_2KE$, ω_1 is continuous, and motion about the other two principle axes is oscillatory. If $L^2 < 2I_2KE$, ω_3 is continuous, and ω_1 and ω_2 are oscillatory. For a symmetrical cylinder ($I_1 = I_2$) in which $I_1 > I_3$, $I_2 < 2I_2KE$, and motion about the roll axis must be continuous. The fact that oscillations rather than rotations are observed about the roll axis indicates the transverse principal axes are distinct; i.e., $I_2 \neq I_1$, and that $L^2 > 2I_2KE$. The solution[3] to the Euler equation for the case considered here may be written (omitting the phase factor)

$$\begin{aligned} \omega_1 &= \alpha dn(pt, k) = \alpha[1 - k^2 sn^2(pt, k)] \\ \omega_2 &= \beta sn(pt, k), \quad \omega_3 = \gamma cn(pt, k) \end{aligned} \tag{4}$$

where sn, cn, and dn are Jacobian elliptic functions and

$$\alpha = \sqrt{\frac{L^2 - 2I_3KE}{I_1(I_1 - I_3)}}, \quad \beta = \sqrt{\frac{2I_1KE - L^2}{I_2(I_1 - I_2)}}$$

$$\gamma = -\sqrt{\frac{2I_1KE - L^2}{I_3(I_1 - I_3)}}$$

$$p^2 = \frac{(L^2 - 2I_3KE)(I_1 - I_2)}{(I_1I_2I_3)}, \quad k^2 = \frac{(2I_1KE - L^2)(I_2 - I_3)}{(L^2 - 2I_3KE)(I_1 - I_2)}$$

Note that the sign of γ must be opposite of that of α and β. The period of oscillation is given by

$$T_0 = 4K(k)/p \tag{5}$$

where $K(k)$ is a complete elliptic integral of the first kind given by

$$K(k) = \int_0^1 \frac{du}{\sqrt{(1 - u^2)(1 - k^2u^2)}}$$

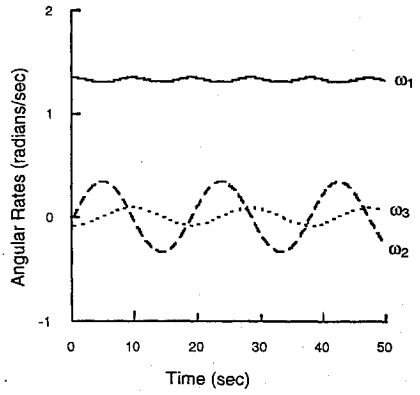

Fig. 3 Computed body rates as a function of time.

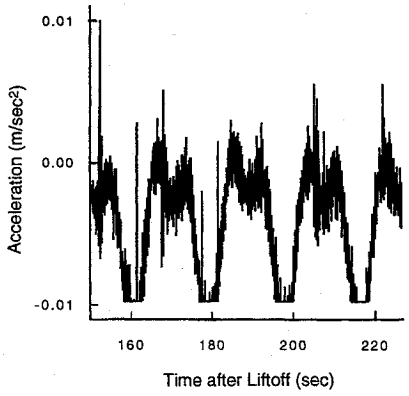

Fig. 4 Observed data from the z-axis accelerometer. The data are clipped at ± 0.01 m/s^2.

As stated previously, neither of the two constants of the motion, L or KE, are known. The moments of inertia about a transverse and the cylindrical or roll axis were measured prior to flight, but it is not known if the measured transverse moment of inertia corresponds to I_1, I_2, or something in between. From geometrical considerations, the cylindrical axis must nearly correspond to the principal axis of least moment of inertia, I_3, and I_2 will be just slightly less than I_1. The solution depends only on the ratios of moments of inertia, and it turns out that because $I_1 \gg I_3$, the solution is relatively insensitive to the ratio of I_3/I_1. (In contrast, the solution was found to be extremely sensitive to I_2/I_1.) Therefore, the measured ratio of axial to transverse moment of inertia can be assumed to be I_3/I_1 without significant error.

From the observed amplitude of the oscillation about the roll axis ($\pm\pi/12$) with a period of 19 s, the maximum amplitude of ω_3 can be determined to be 0.0865 rad/s, which gives a value of -0.0865 for γ. However, because the reference gyro data were clipped at ± 28 deg, there is no good estimate of the ω_2 amplitude. Furthermore, only the average value for ω_1 is known.

The equations for p and k can be combined to eliminate $L^2 - 2I_3KE$ and the value determined for γ can be used to eliminate $2I_1KE - I^2$ giving

$$p^2k^2 = \frac{(2I_1KE - L^2)(I_2 - I_3)}{(I_1I_2I_3)} = \frac{(1-C)(B-C)\gamma^2}{B} \tag{6}$$

Similarly the equation for the amplitude of ω_1 may be written as

$$\alpha^2 = p^2\frac{BC}{(1-B)(1-C)} \tag{7}$$

from which the average rate for ω_1 can be found by integrating

$$\bar{\omega}_1 = \frac{\alpha}{T_0}\int_0^{T_0}\left[1 - k^2 sn^2(pt,k)\right]dt \tag{8}$$

The task now is to find values for B, p, and k so that Eq. (5) yields the observed period of oscillation, Eq. (8) predicts the observed average value for ω_1, and the relationship given by Eq. (6) is satisfied. Because these equations are nonlinear and transcendental, an iterative approach is required. The following procedure was used.

1) A value of B ($1 > B > 0$) was selected. A value for $(pk)^2$ was computed from Eq. (6), using the known value for C and γ.

2) A value for the modulus k ($1 > k > 0$) was selected, and p was computed from the product obtained in step 1.

3) The period of oscillation was computed from Eq. (5). Step 2 was repeated with different values of k until the observed value for T_0 was obtained.

4) The value for α was computed from Eq. (7) and used to carry out the integration in Eq. (8) to obtain the average ω_1. The procedure was repeated from step 1 with different values for B until the observed value for $\bar{\omega}_1$ was obtained.

The iterative procedure is greatly simplified by the fact that both B and k are bounded by 0 and 1 and because the vehicle is nearly symmetrical, $B \approx 1$. Having determined the value for B consistent with the observed motion, the amplitude for ω_2 can be determined by using the value of γ to eliminate $2I_1KE - L^2$ in the expression for β giving

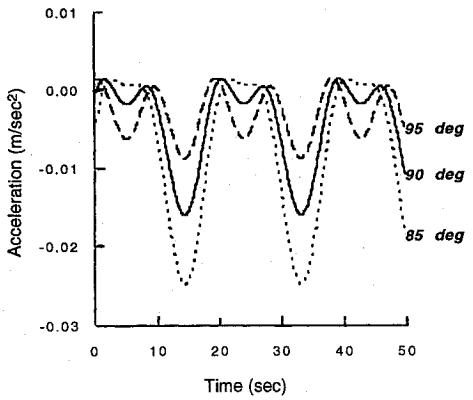

Fig. 5 Computed z-accelerations for small variations of ν around 90 deg.

$$\beta^2 = \gamma^2\frac{C(1-C)}{B(1-B)} \tag{9}$$

Now the body rates and their derivatives can be determined to within an arbitrary phase factor. However, there is still the problem of orienting the transverse principal axes I_1 and I_2 relative to the vehicle coordinates. The body rates can be projected on the vehicle coordinates by

$$\omega_x = \omega_3,\ \omega_y = \omega_1\cos\nu - \omega_2\sin\nu,\ \omega_z = \omega_1\sin\nu + \omega_2\cos\nu \tag{10}$$

where n is to be determined by matching the computed acceleration vector against the accelerometer data.

Results

For $C = 0.009$ and $\gamma = -0.0865$ rad/s, the value $B = 0.99944$ was found to produce $k = 0.255$, $p = 0.3361$/s, and $\bar{\omega}_1 = 1.34$ rad/s. From this, $\alpha = 1.353$ rad/s and $\beta = 0.3453$ rad/s. The $2KE/I_1 = 1.83168/s^2$, while the $L^2/I_1^2 = 1.83162/s^2$, but the product $2BKE/I_1 = 1.83066/s^2$, which satisfies the requirement $L^2 > 2I_2KE$. The resulting body rates are shown in Fig. 3.

The z-axis accelerometer provided the most interesting and useful data for obtaining the proper transformation angle because it was offset from the x-axis in both the y- and z-directions. Its position vector $\boldsymbol{r} = (0.608, 0.017, -0.074)$ m in vehicle coordinates. The observed acceleration exhibited a peculiar double hump, as shown in Fig. 4.

This pattern is faithfully reproduced in the acceleration computed from Eq. (1) using the body rates and their derivatives obtained from Eq. (6), and taking the transformation angle $\nu = 90$ deg. Even small deviations from this value of ν give dramatically different

patterns, as can be seen in Fig. 5. Choosing $\nu = 270$ deg gives a similar pattern, but the position of the large and small humps are interchanged; hence, even the sense of the rotation can be obtained from the accelerometer data. Similar agreement was obtained for both the x- and y-axis accelerometers.

Conclusion

A solution to the full set of Euler equations for a tri-axial rigid body was obtained knowing only the ratio ofthe minimum to the maximum moment of inertia, the average rate of tumble, and the amplitude and period of the rocking motion about the roll axis. The constants of motion L and KE and the moment of inertia about the intermediate principal axis were deduced by an iterative solution to the highly nonlinear set of equations that represent the closed form solution to the Euler equations. The body rates and their derivatives obtained from this solution were then used to compute the acceleration environment throughout the vehicle. Excellent agreement was obtained with the accelerometer data taken at one point in the vehicle. This makes us confident that the computed acceleration environment is correct, and it demonstrates that acceleration mapping can be accomplished.

References

[1]Wessling, F. C., and Maybee, G. W., "Consort 1 Sounding Rocket Flight," *Journal of Spacecraft and Rockets*, Vol. 26, No. 5, 1989, pp. 343–357.

[2]Bijvoet, J. A., Wingo, D. R., Radorf, J., and Blakely, J. R., "Advances on Relative and Absolute Microgravity Measurements in Space and Flight Results," International Astronautical Federation, IAF Paper 9290967, Sept. 1992.

[3]Synge, J. L., and Griffith, B. A., *Principles of Mechanics*, 3rd ed., McGraw-Hill, New York, 1959, p. 378.